Atmos. Chem. Phys. Discuss., 4, 6909–6941, 2004
www.atmos-chem-phys.org/acpd/4/6909/
SRef-ID: 1680-7375/acpd/2004-4-6909

Atmospheric Chemistry and Physics Discussions

Pole-to-pole validation of GOME WFDOAS total ozone with groundbased data

M. Weber, L. N. Lamsal, M. Coldewey-Egbers, K. Bramstedt, and J. P. Burrows

Institute of Environmental Physics, University of Bremen, Bremen, Germany

Received: 10 June 2004 – Accepted: 18 August 2004 – Published: 29 October 2004

Correspondence to: M. Weber (weber@uni-bremen.de)

Abstract

This paper summarises the validation of GOME total ozone retrieved using the weighting function differential optical absorption spectroscopy (WFDOAS) algorithm Version 1.0. This algorithm has been described in detail in a companion paper by Coldewey-Egbers et al. (2004). The WFDOAS results have been compared with selected ground-based measurements from the WOUDC (World Ozone and UV Radiation Data Centre) that collects total ozone measurements from a global network of stations covering all seasons. From the global validation excellent agreement between WFDOAS and ground data was found and on average agree to within ±1%. Very little seasonal variations in the observed differences are observed. In the polar region and at high solar zenith angles, however, a positive bias varying between 5 and 8% is found. Very few stations carry out simultaneous measurements by Brewer and Dobson spectrometers over an extended period (three years or more). Simultaneous Brewer and Dobson measurements from Hradec Kralove, Czech Republic (50.2° N, 15.8° E) and Hohenpeissenberg, Germany (47.8° N, 11.0° E) covering the period 1996–1999 have been compared with our GOME results. Agreement with Brewers are generally better than with the simultaneous Dobson measurements and this may be explained by the neglect of stratospheric (ozone) temperature correction in the standard ozone retrieval from the ground.

1. Introduction

The GOME (Global Ozone Monitoring Experiment) on board the ERS-2 satellite is the first European experiment dedicated to global ozone measurements (Burrows et al., 1999a). It measures the back scattered radiances from 240–790 nm in the nadir-viewing geometry. In the relevant region for total ozone retrieval (320–340 nm) the spectral resolution is about 0.17 nm. The maximum scan width in the nadir is 960 km across track on the ground and global coverage is achieved within three days.

For the major parts of the orbits one across track scan sequence consists of four ground pixel types with 1.5 s integration time each and ground coverage is 320 km by 40 km. The GOME instrument aboard ERS-2 provides regular solar irradiance and backscatter spectra starting in July 1995. In June 2003 the tape recorder for intermediate data storage failed, so that only data are transmitted to the ground when ERS-2 is in direct contact with ground stations. This limits GOME coverage to the Euro-Atlantic sector stretching from Canada to Russia.

In a companion paper (Coldewey-Egbers et al., 2004) a new total ozone retrieval algorithm has been introduced that uses the weighting function differential optical absorption spectroscopy (WFDOAS) approach. It introduces several new features that lead to higher sensitivity to clouds and properly accounts for the ozone dependent contribution to the Raman scattering responsible for the filling-in of molecular absorption. This paper describes the validation of WFDOAS with groundbased data on a global scale.

In Sect. 2 the WFDOAS algorithm is briefly summarised. In Sect. 3 comparison with simultaneous Brewer and Dobson measurements at Hohenpeissenberg (47.8° N, 11.0° E) and Hradec-Kralove (50.2° N, 15.8° E) are presented and discussed. This is a very important comparison since many stations are changing from regular Dobson to Brewer observations and a good characterisation of satellite data with respect to both spectrophotometer types is critical for long-term trend assessment from both satellite and ground time series (Staehelin et al., 2003). The following section summarises the global comparison between WFDOAS and 45 ground stations from the WOUDC database. A detailed comparison for all latitude bands (in steps of 30°) is provided (Sect. 4). Most of the validation statistics relied on ground-based data between 1996 and 1999. For one station as an example (Lauder in New Zealand) the comparison has been extended well into 2003 and results are presented in Sect. 6.

ACPD
4, 6909–6941, 2004

2. WFDOAS algorithm

In the WFDOAS algorithm the measured atmospheric optical depth (logarithm of the sun-normalised radiances) is approximated by a Taylor expansion around a reference intensity plus a low-order polynomial, here a cubic polynomial. The total column information is obtained only from differential trace gas structures as in case of standard DOAS and the polynomial accounts for all broadband contributions from surface albedo and aerosol.

Additional fit parameters are the Ring effect, the undersampling correction, both treated as effective absorbers similar to the approach used in standard DOAS, and a (ozone) temperature shift. Slant column fitting is also applied to the minor absorbers NO_2 and BrO. All fitting parameters are derived using a linear least squares minimization. A large set of reference spectra has been constructed that includes nearly all possible atmospheric conditions. The radiance spectra and weighting functions were calculated as a function of total ozone including profile shape, solar zenith angle, line-of-sight, relative azimuth angle, and bottom-of-atmosphere altitude and albedo using the multiple scattering SCIATRAN radiative transfer model in the pseudo-spherical approximation (Rozanov et al., 1998).

Ozone and temperature profiles are taken from TOMS V7 climatology (Wellemeyer et al., 1997) which contains different profile shapes for three latitude belts (low, middle and high) as a function of total ozone column varying from 125–575 DU in mid and high latitudes and from 225–475 DU in low latitudes. Solar zenith angle varies from 15°–92°, line-of-sight varies from −34.5° to +34.5°, and the range for the relative azimuth angle is defined by a given combination of both parameters. Altitude of the boundary in the lower atmosphere varies from 0 to 12 km, and surface albedo from 0.02 to 0.98. Both parameters are considered effective parameters that take into account partial cloud cover in the GOME scene.

For ozone retrieval with WFDOAS calibrated GOME level 1 radiance and solar spectrum from the same day, a-priori values for total ozone (initial guess), effective altitude,

ACPD
4, 6909–6941, 2004

GOME WFDOAS total ozone validation

M. Weber et al.

and effective albedo are used. Effective altitude is obtained from FRESCO (Fast Retrieval Scheme for Clouds from the oxygen A-Band, Koelemeijer et al., 2001). Cloud top pressure and cloud fraction are derived from the oxygen transmittance assuming a high reflecting boundary representing the cloud top. Surface albedo is taken from minimum spectral reflectances derived from a five year GOME data record (Koelemeijer et al., 2003). The effective height is the sum of the ground altitude and the retrieved cloud top height weighted by the fractional cloud cover (Coldewey-Egbers et al., 2004).

The Lambertian Equivalent Reflectivity LER (Herman and Celarier, 1997) defines the effective albedo and is obtained from GOME sun-normalized radiances at 377.6 nm, where variations with respect to the Ring effect are small and can be easily corrected for. A look-up-table of radiances as a function of solar zenith angle, line-of-sight, relative azimuth angle, ground altitude, and surface albedo has been pre-calculated using SCIATRAN and the LER are retrieved by finding the best match between calculated and measured TOA reflectance by inverse search in the multidimensional table.

As described in Coldewey-Egbers et al. (2004) the Raman correction to scattered intensity, the so-called Ring spectra (Solomon et al., 1987; Vountas et al., 1998), were calculated for the same atmospheric conditions including ozone variability as provided by the profile shape climatology as for the weighting functions and are stored in look-up tables (LUT). The spectral window 326.8–335.0 nm is used in the ozone fitting procedure. After the iteration stops, the ghost vertical column (GVC), that is hidden below the (partial) cloud, is determined from an ozone climatology and then added to the retrieved column to obtain the final total ozone amount. The tropospheric climatological ozone is taken from the monthly and zonal mean TOMS V8 profile climatology (G. Labow, NASA GSFC, personal communication).

The following settings apply to Version 1.0 WFDOAS:

- spectral fitting window: 326.8–335.0 nm
- fitting terms:
  - ozone vertical column (WF)

  - temperature shift (WF)
  - under-sampling correction
  - Ring (including ozone filling-in)
  - NO_2
  - BrO
- a-priori ozone profile shape from total ozone dependent TOMS V7 ozone and temperature climatology (Wellemeyer et al., 1997)
- Burrows et al. (1999b) ozone cross-section shifted by +0.017 nm
- Fraunhofer fitting (wavelength calibration of daily solar GOME reference to Kitt Peak Fourier transform solar atlas from Kurucz et al., 1984)
- shift and squeeze of wavelength axis only for nadir radiance spectrum
- cubic polynomial subtracted in the fit
- Lambertian equivalent reflectivities (377.6 nm) taken as effective albedo of the scene
- cloud-top-height and cloud cover fraction derived using FRESCO (Koelemeijer et al., 2001). Effective scene height is determined from the cloud-information
- ghost vertical column correction from TOMS V8 zonal monthly mean climatology

The Fraunhofer fitting and the spectral shift of the ozone cross-section used in the radiative transfer calculation permits the limitation of wavelength adjustments (shift and squeeze) to the GOME nadir radiances. This leads to a faster retrieval on the order of five minutes per GOME orbit (about 1500 fits).

ACPD

4, 6909–6941, 2004

3. GOME, Brewer, and Dobson triple comparison

The majority of the total ozone data obtained from the ground are Dobson spectrophotometer measurements. The Dobson spectrophotometer is a double monochromator with the first prism acting as a dispersing element and the second recombining the wavelength pair on to a photomultiplier. A chopper allows the alternating measurements of the wavelength pair with a single detector (Dobson, 1931, 1968). For the standard analysis (World Meteorological Organization – Global Atmospheric Watch (WMO-GAW)) the A (305.5/325.5 nm) and D (317.6/339.8 nm) wavelength pairs are used to derive total ozone (Staehelin et al., 2003). At low solar elevation the D-pair can be combined with the C-pair 311.5/332.4 nm. This instrument can be operated in direct-sun and zenith sky viewing geometry. Most reliable results are obtained in direct-sun (AD pairs) with a precision of 1% using a diffuser plate. Accuracy may be lower due to systematic errors, for instance coming from uncertainties in cross-sections (Bass-Paur are used in the standard retrieval). Under cloudy conditions the error in the zenith-sky results can rise from 3% up to 7% (low clouds) in zenith sky measurements (R. D. Evans, NOAA, personal communication). First measurements with the Dobson instruments have been reported in the twenties (Dobson, 1931) and some of the longest time series are provided by the Dobson instruments (Staehelin, 1998).

Since the early eighties Brewer grating spectrometers have been installed at several stations (Kerr et al., 1985). It is a modified Ebert type grating spectrometer which can be operated in single ("single Brewer") or double monochromator ("double Brewer") configuration. This instrument uses five wavelengths in the spectral range 306.3 and 320.1 nm to form several wavelength pairs for the standard ozone retrieval. Besides ozone, NO_2, SO_2, and UV-B radiation can be measured. Particularly SO_2 interferes in the ozone retrieval and has to be corrected for in an urban environment. Both direct-sun and zenith-sky measurements are possible.

Only very few stations provide simultaneous measurements from Brewer and Dobson spectrometers covering an extended period. Two such stations are Hohenpeissenberg (MOHp), Germany, 47.8° N, and Hradec-Kralove, Czech Republic, 50.2° N. Both stations in collaboration act as the Regional Dobson Calibration Centre for Europe. They have been operating a single Brewer and Dobson throughout the GOME period 1995–2003 and this data set is very valuable in evaluating the new GOME algorithm. Because of different wavelengths used in all three instruments GOME, Brewer, and Dobson, results may differ. Also seasonal dependence on the retrieved ozone may differ. The standard retrieval procedure as defined by WMO-GAW, for instance, does not correct for the ozone temperature variation in contrast to the GOME retrieval.

For both stations a maximum collocation radius of 160 km between the center of the GOME pixel and station location was allowed and measurements had to take place the same day. At a given day only the closest match within that radius was taken. Brewer and Dobson data were provided as daily averages. All Dobson measurements and the Hradec-Kralove Brewer are limited to direct sun measurements that are considered most reliable. Hohenpeissenberg Brewer data also contain zenith-sky measurements.

Figure 1 shows the comparison between WFDOAS V1.0 and Hohenpeissenberg Brewer as a function of the day in the year (1996–1999). The top panels shows the annual cycle of total ozone with maximum ozone in spring and minimum in fall, the bottom panel the difference in percent. The WFDOAS results have a bias of 0.4% and a ±0.5% variability over the annual cycle with slightly higher values in winter (JFM) than in summer/fall. The 1σ RMS in the differences is 2.3%.

The comparison of the GOME WFDOAS V1.0 with the Dobson measurements is shown in Fig. 2. The RMS scatter in the differences are similar for both Brewer and Dobson data (2.3% and 2.9%, respectively). WFDOAS exhibits a somewhat stronger seasonal cycle of ±1% when compared to Dobson with a maximum of +1.5% during winter and 0% difference in summer. WFDOAS results appear to exhibit only a very small seasonal variation with respect to the Brewer.

Similar conclusions can be derived from the comparison with the ground-based data from Hradec-Kralove. In Fig. 3 different combinations of differences between satellite and ground-based data are shown. The top two panels show differences of WFDOAS with respect to Brewer and Dobson, while the lowermost panel depicts the differences between average Dobson and Brewer results from the same day.

The WFDOAS bias with respect to Brewer is less than 0.2% and the very weak seasonal cycle of ±0.5% like in the MOHp data is evident here. A somewhat larger seasonal variation is observed if compared to Dobson (±1%). This is in line with the earlier comparison to MOHp. Note that the percentage scale is larger in these plots as compared to the MOHp plots; the RMS scatter of the differences remains about the same.

When comparing data from both stations it is noticeable that the Hradec-Kralove Dobson is 0.5% lower on average than the same instrument at MOHp. A new set of calibration settings were introduced in Hradec-Kralove in 1997 that were not adopted at MOHp (U. Köhler, DWD, personal communication, see also Staehelin et al., 2003) and that may explain this bias. The change in the calibration settings is also noticeable from the longterm times series in the Dobson-Brewer differences at Hradec-Kralove that showed less variability in 1996 and earlier (Staehelin et al., 2003, see Fig. 5).

A distinct seasonal cycle in the Dobson-Brewer differences is noticed with maxima in winter and minimum (near zero) in summer. The major contribution to this seasonal cycle in Dobson-Brewer differences is due to the use of different wavelength pairs in both instruments to retrieve ozone. Particularly, the D pair ratio of the O_3 cross-sections (317.6/339.8 nm) as used by the Dobson shows the largest temperature dependence of all ratios used in the standard retrieval by both instruments (Staehelin et al., 2003). However, a fixed temperature (226.9 K) ozone cross-section is applied in the standard retrieval so that stratospheric temperature variation with season is not accounted for. During winter the stratospheric temperature are well below 226.9 K that may explain the larger differences between Dobson and Brewer. For a typical ozone/temperature variability at mid-latitude station a sensitivity of +1.3%/10 K and +0.7%/10 K in ozone change for Dobson and Brewer, respectively, has been estimated (Komhyr et al., 1993; Kerr et al., 1988). Due to the reduced temperature sensitivity of the Brewer wavelengths, it is not unexpected that GOME WFDOAS agrees better with Brewer. It should be also noted that the temperature sensitivity is also larger with direct sun than with zenith sky ground-based observations (Vanicek, 1998).

4. Pole-to-pole validation

Forty-five stations have been selected from the WOUDC data base (Hare and Fioletov, 1998; Fioletov et al., 1999) for validating WFDOAS V1.0. The stations are summarised in Table 1. Only those stations have been selected that show no larger gaps in time and do not suffer from unreasonable jumps in short time and do not have an average bias clearly exceeding 5%. Particularly at northern hemispheric mid latitudes, many more stations were available but a fairly even distribution in longitudes were ensured by selecting 19 stations out of this data set. The majority of data are from Dobson measurements. The maximum collocation radius was here set to 300 km (between centre of GOME footprint and station) and only the nearest GOME overpass was used at given day. The same data set has been used in a recent paper validating the GOME V2.7 data version (Bramstedt et al., 2003). For each climate zone (in 30° steps) a representative station has been selected and the differences are shown as a function of time from 1996 to 1999 in Fig. 4. The stations are from north to south; Resolute (Canada, 75° N), Boulder (USA, 40° N), Singapore (1° N), Comodoro Rivadavia (Argentina, 46° S), and Syowa, the Japanese station in Antarctica (69° S). Also shown are the three month mean time series (orange line) in order to visualize possible seasonal variability and a longterm drift in the data. Data shown here have been analyzed with the appropriate ozone profile climatology (tropics, mid-latitude, and polar). As with earlier versions of the GOME total ozone and in the previous sections, the time series of satellite-station differences show no significant long-term drift (GDP V3 VALREPORT, 2002; Bramstedt et al., 2003).

Both mid-latitude stations in both hemispheres as well as the data from Singapore have an average bias over the four year period that is well below ±0.5%. Except for Boulder and the polar stations no seasonal signature is detectable. The Boulder dif-

ACPD

4, 6909–6941, 2004

ference series has a distinct seasonal cycle of up ±1.5% starting in 1997 that is not apparent in 1996. As discussed in the previous section it could be related to the change in calibration settings that many stations introduced to their Dobson spectrophotometers in 1997. The seasonal signature in Boulder is quite similar to that observed with Hradec-Kralove and MOHp Dobsons with maximum in northern hemispheric winter (January, February, March) and minimum in summer (July, August, September).

In Comodoro Rivadavia, Argentina, a seasonal signature is not clearly discernible, except for occasional larger deviations that are not repeated in other years. This is most likely related to interruptions in measurements in southern hemispheric summer (January, February, March), so that only few data contributed to the three month average as in 1997 and 1999.

The two stations in the south and north polar region, Syowa and Resolute, show a distinct annual cycle in the GOME-Dobson differences. Average differences in spring/summer are quite low (below 1%) but can increase to +5% close to the polar night terminator. It is noted that this pattern is symmetric about the polar night period, although total ozone under ozone hole conditions in spring is much lower than in fall. The large gradients in ozone observed near the polar vortex edge is responsible for the larger scatter in the SH spring, because both GOME and surface instrument do not look at the same airmass. In Sect. 5 the validation in polar region under ozone hole condition is discussed in more detail.

For the statisticial analysis the GOME total ozone was retrieved twice using two different profile shapes for each climate zone. At mid- to high latitudes the TOMS V7 profile shape from both climate zones were applied in each region (WFD-HI and WFD-MI). In the tropics low- (WFD-LO) and mid-latitude ozone profiles were selected. In order to evaluate the spread of the various station data the 1σ RMS of the scatter for the mean differences has been determined and the 2σ range is indicated in the plots (only for default WFD climatology matching the climate zone). A comparison between the current official data version called GOME Data Processsor V3 (short: GDP V3) and the groundbased data have also been included in order to visualise the changes between the two retrievals. A detailed description of GDP V3 can be found in GDP V3 VALREPORT, 2002.

A plot summarizing the comparison between different analysis, GDP V3, WFD-HI, and WFD-MI with nineteen mid-latitude stations is shown in Fig. 5. The average annual bias is −0.4% for WFD-MI, the default analysis for this latitude band. A small seasonal variation of about ±0.5% can be seen, with maximum in winter and minimum in summer statistically confirming the results from the individual station comparison. If the high-latitude profiles are used the seasonal variability doubles to ±1% with a lower annual bias. The GDP V3.0 shows an annual variability of ±1% with a bias of around −1% with respect to the station data. However, the maximum and minimum in the GDP difference are shifted towards spring (maximum) and fall (minimum).

By looking at individual mid-latitude stations, it can be noted that for some stations the seasonal variation is absent (e.g. Dobsons in Uccle, Belgium, and Lauder, New Zealand), while for other stations a weak seasonal cycle is observed with WFDOAS. In order to see the effect on the statistics by selecting different stations, the comparison has been limited to eight European stations (Arosa, Lindenberg, Potsdam, Hohenpeissenberg, Hradec-Kralove, Uccle, Camborne, and Oslo) and Russian stations that mainly operate the so-called M-124 filter spectrometers to measure ozone (Gushchin et al., 1985) have been excluded. Almost no seasonal variation is observed in the WFD-MI mean differences to the European stations, while the seasonal cycle in the GDP V3 differences still remains as shown in Fig. 6.

The annual course of the GOME differences to the ground-based data for tropical and SH mid latitude stations (see Table 1) is shown in Fig. 7. The SH mid-latitude differences show a similar pattern (now shifted by six month) as observed in the NH (Fig. 5). The default WFD-MI differences like in the NH mid latitudes show no significant annual cycle. The mean bias in low and mid-latitudes is less than 0.5% for WFDOAS V1.0 using the appropriate ozone profile shapes (default retrieval). Using a profile shape from a neighboring climate zone leads in general to worse agreement with ground data.

ACPD

4, 6909–6941, 2004

Figure 8 shows the results from the polar regions. The southern hemispheric data show on average a difference of four percent with respect to ground-based data near the polar night period, in some winters it can reach 10% like during Antarctic spring 1997. Over the annual cycle the average bias is about 1%. This comparison is difficult since solar elevation angles are low and large gradients near the polar vortex edge leads to the huge scatter in the RMS which can reach a 2σ value of 40%.

Similar arguments apply to the NH polar stations but not as extreme as in the SH (see Fig. 8). The seasonal variation in the differences for both WFDOAS and GDP is very similar to the one observed at mid-latitudes, but enlarged. It appears that in all GOME analyses the winter differences has increased from 1996 up to 1999. It is known that the NH polar ozone shows large interannual variability inside and outside of the polar vortex (see for instance Weber et al., 2002, 2003). The Arctic winter 1997/1998 and 1998/1999 have been rather warm stratospheric winters with high ozone beyond 50 DU, while 1996/1997 marked the end of a series of cold stratospheric Arctic winters in the mid-nineties with lower winter total ozone levels. It appears that at low solar elevation and higher total ozone the winter differences are closer to 5% (1998/1999) and otherwise closer to +2 to +3%. The apparent trend seen in the top right panel in Fig. 8 may be therefore accidental.

At low solar elevation Dobson instruments suffer from forward scattered stray light and therefore may underestimate the total column. At the same time the intensity of the scattered light decreases and signal-to-noise increases in the GOME radiances and error also gets larger. It is generally difficult for UV/vis instruments to operate in near twilight condition. To reach a better understanding of differences between satellite (TOMS) and ground-based instruments at high-latitudes a measurement campaign involving two Dobson and three Brewer instruments were carried out in Fairbanks, Alaska, in March/April 2001. Against the world standard (Instrument D83, AD pair, direct sun), all Brewer instruments as well as integrated sonde profiles have shown a percent difference of +3 to +4% with respect to the world standard (Staehelin et al., 2003). The Fairbanks direct-sun Dobson results showed a difference of −1.3% using

ACPD
4, 6909–6941, 2004

the AD pair and, when using proper ozone temperature and the CD Pair, a +3.5% difference with respect to D83 was found. In winter/early spring 1998 and 1999, Arctic ozone levels were similar to those in 2001 during the TOMS3-F campaign. and a WFDOAS difference of +2 to +4% is observed in late winter/early spring with respect to the Resolute Dobson, that goes in the same direction as the differences observed in Fairbanks.

5. Validation under ozone hole condition

Particular interest in total ozone monitoring is the development of the Antarctic ozone hole from year-to-year. In the WOUDC statistics four stations from Antarctica have been included for the SH polar stations. It was found that close to the polar night period GOME WFDOAS V1 as well as GDP V3.0 can be up to 10% higher on average than ground based Dobson. However the variability of the differences is also very large, so that the differences observed may be also to a large extent depend on the station. In Fig. 9 the results from GOME WFDOAS and Dobson comparison for each of the four Antarctic stations, Syowa, Halley Bay, Marambio, and Arrival Heights, are shown as a function of solar zenith angle and GOME total ozone covering the 1996–1999 period.

The large scatter in the observed differences from Arrival Heights and Marambio are clearly observed. The Halley Bay and Syowa differences show a slight upward trend of up to 5% near 90° solar zenith angle. Except for the lowest total ozone as observed at Halley Bay with values near 10% (below 140 DU) there appears only a weak dependence on total ozone. It should be noted that for GOME total ozone above 250 DU similar differences are observed as for the lowest ozone values below 140 DU at Halley Bay. This may indicate that the apparent trend in Fig. 9 is related to the solar zenith angle dependency rather than to total ozone. This is also consistent with larger differences between WFDOAS V1.0 and Dobson observed in late fall well before the large scale ozone depletion starts (see Fig. 8; bottom left panel).

6. Longterm validation 1996–2003

A long-term comparison has been carried out with the Dobson data from Lauder, 45° S, and Hohenpeissenberg, 48° N. The WFDOAS time series along with the Lauder Dobson data is shown in Fig. 10. The Hohenpeissenberg time series has been shown in Fig. 7 of Coldewey-Egbers et al. (2004). All Lauder measurements from zenith-sky and direct-sun groundbased data have been included. Apart from a bias of +0.4% for the entire time period (identical to the bias observed in Hohenpeissenberg) no seasonal variation is seen in the comparison with WFDOAS V1.0. The bottom panel in Fig. 10 shows the same comparison but with GDP V3.0, where a distinct seasonal cycle is evident for all years. From this limited comparison up to 2003, it can be concluded that the DOAS retrieval does not suffer from the optical degradation that have altered the radiometric accuracy of the GOME instrument particularly in later years (Tanzi et al., 2001).

7. Conclusions

The new WFDOAS algorithm for GOME has been extensively compared with globally distributed ground-based data, predominantly Dobson spectrophotometer data. In mid-latitudes it agrees on average to within half a percent with the WOUDC data. A small seasonal variation of about ±0.5% is noted, with a maximum in the differences in fall/winter and a minimum in spring/fall. At many mid-latitude stations, e.g. Lauder and Uccle, no seasonal variation is observed. GDP V3 clearly shows a larger annual variation (±1%) but the maximum in the differences is shifted towards spring (minimum in fall). No major changes are observed with the new WFDOAS in the tropics, a constant bias between WFD-DOAS (below +1%) and GDP (about −1%) with respect to the ground-based data throughout all years are observed.

In the polar region larger positive differences are observed with WFDOAS at high solar zenith angles (up to 4%). If comparisons are made near the polar vortex edge

ACPD

4, 6909–6941, 2004

errors can get quite large (up to 40%). If both GOME and the station are well inside the ozone hole it appears that the differences are below 5%.

The comparison with the Brewer instruments at Hradec-Kralove and Hohenpeissenberg has demonstrated excellent agreement with WFDOAS. The maximum in the differences between GOME and Dobson and to a lesser extent with Brewer is related to the fixed ozone temperature used in the standard retrieval of the ground-based instruments. Brewer-Dobson differences can be as high as ±2% (generally on the order of 0.5%). This variability gets maximum at high latitudes due to lower solar elevation and the enhanced stray-light problem associated with it. The Fairbanks campaign TOMS3-F, where differences of up to 3–4% between ozone temperature corrected Brewer and standard Dobson were measured in late winter, seem to support this conclusion (Staehelin et al., 2003). The closer agreement of WFDOAS with Brewer than simultaneous Dobson data confirm that the temperature shift weighting function appears appropriate to account for the ozone temperature variation.

The TOMS V7 climatology (Wellemeyer et al., 1997) seems to work well in WFDOAS V1.0. Using a false climate zone (mid-latitude profiles in polar region, for instance) seems still to provide very reasonable results but make generally the comparison to ground-based data slightly worse and increases the seasonal variability somewhat. Particularly, the mid-latitude TOMS V7 ozone profiles can be globally applied in the retrieval except in polar regions at high solar zenith angles where differences become more distinct. The largest differences are also to be expected at moderate low ozone 220–280 DU when two types of profile shapes produce the same ozone column density, namely a weakly ozone depleted ozone hole profile and a high tropopause profile. Both can be observed frequently at mid- to high latitudes.

Overall it can be concluded that the accuracy of the WFDOAS V1.0 results are now within the uncertainty of the ground-based measurements. The very good agreement with ground based instruments are proof that several issues that has been newly introduced in WFDOAS V1.0 have drastically improved total ozone retrieval: 1) ozone filling-in as part of the Ring effect, 2) the introduction of an effective scene height from cloud information and 3) derivation of an effective scene albedo from the GOME spectral measurements. These changes are, however, not specific to the type of algorithm that has been used here but can be potentially applied to other retrieval schemes as well. The WFDOAS theoretical approach by expanding the differential optical depth equation in a Taylor series is a straight forward formulation of the DOAS inversion and is applicable in a more general way than the standard DOAS approach that uses airmass factors to correct for the slant path geometry like in earlier GOME versions. This algorithm can be also applied to other UV/vis backscatter satellite instruments such as SCIAMACHY (Bovensmann et al., 1999) and OMI (Laan et al., 2000) that measure in continous scan mode.

Acknowledgements. We thank U. Köhler and H. Claude, MOHp Heissenberg, for providing us with their station data (Brewer and Dobson) and for their insights into the ground-based measurements. We also thank B. Evans, NOAA, for providing us data from Lauder and he kindly informed us on the accuracy of the Dobson spectrophotometers. K. Vanicek, Czech Hydrometeorological Institue, kindly provided Brewer and Dobson data from Hradec Kralove. We also thank him for giving us valuable information on the groundbased data. This project was supported in parts by European Space Agency contract 16402/02/I-LG, BMBF grant 7ATF42 (GOMSTRAT) within the AFO2000 national research programme, and EU project EVK2-CT-2001-00133 (CANDIDOZ).

References

Bovensmann, H., Burrows, J. P., Buchwitz, M., Frerick, J., Noel, S., Rozanov, V. V., Chance, K. V., and Goede, A. H. P.: SCIAMACHY – Mission Objectives and Measurement Modes, J. Atmos. Sci., 56, 125–150, 1999. 6925

Bramstedt, K., Gleason, J., Loyola, D., Thomas, W., Bracher, A., Weber, M., and Burrows, J. P.: Comparison of total ozone from the satellite instruments GOME and TOMS with measurements from the Dobson network 1996–2000, Atmos. Chem. Phys., 3, 1409–1419, 2003. 6918

Burrows, J. P., Weber, M., Buchwitz, M. Rozanov, V. V., Ladstädter-Weissenmayer, A., Richter, A., de Beek, R., Hoogen, R., Bramstedt, K., Eichmann, K.-U., Eisinger, M., and Perner, D.: The Global Ozone Monitoring Experiment (GOME): Mission Concept and First Scientific Results, J. Atmos. Sci., 56, 151–175, 1999a. 6910

Burrows, J. P., Richter, A., Dehn, A., Deters, B., Himmelmann, S., Voigt, S., and Orphal, J.: Atmospheric Remote-Sensing Reference Data from GOME: Part 2. Temperature-dependent absorption Cross Sections of O_3 in the 231–794 nm range, J. Quant. Spectrosc. Rad. Transfer, 61, 509–517, 1999b. 6914

Coldewey-Egbers, M., Weber, M., Lamsal, L. N., de Beek, R., Buchwitz, M., and Burrows, J. P.: Total ozone retrieval from GOME UV spectral data using the weighting function DOAS approach, Atmos. Chem. Phys. Discuss., 4, 4915–4944, 2004. 6910, 6911, 6913, 6923

Dobson, G. M. B.: A photo-electric spectrometer for measuring the amount of atmospheric ozone, Proc. Phys. Soc., 324–339, 1931. 6915

Dobson, G. M. B.: Forty year's research on atmospheric ozone at Oxford: a history, Appl. Opt., 387–405, 1968. 6915

Fioletov, V., Kerr, J., Hare, E., Labow, G., and McPeters, R.: An assessment of the world ground-based total ozone network performance from the comparison with satellite data, J. Geophys. Res., 104, 1737–1748, doi:10.1029/1998JD100046, 1999. 6918

GDP V3 VALREPORT, 2002: ERS-2 GOME GDP 3.0 Implementation and Delta Validation Report, Technical Note ERSE-DTEX-EOAD-TN-02-0006, Issue 1.0, edited by Lambert, J.-C., November 2002, see also: http://earth.esrin.esa.it/pub/ESA_DOC/GOME/gdp3/gdp3.htm, 2002. 6918, 6920

Gushchin, G. P., Sokolenko, S. A., and Kovalyov, V. A.: Total-ozone measuring instruments used at the USSR station network, in Atmospheric Ozone, edited by Zerefos, C. and Ghazi, A., 543–546, Commission of the European Communities, Reidel, Dordrecht, 1985. 6920

Hare, E. and Fioletov, V.: An examination of the total ozone data in the World Ozone and Ultraviolet Radiation Data Center, in Atmospheric Ozone – Proc. 18th Quadrennial Ozone Symposium, L'Aquila, Italy, edited by Bojkov, R. and Visconti, G., 45–48, 1998. 6918

Herman, J. R. and Celarier, E. A.: Earth surface reflectivity climatology at 340–380 nm from TOMS data, J. Geophys. Res., 102, 28 003–28 011, 1997. 6913

Kerr, J. B., McElroy, C. T., Wardle, D. I., Olafson, R. A., and Evans, W. P. J.: The automated Brewer Spectrophotometer, in Atmospheric Ozone, edited by Zerefos, C. S. and Ghazi, A., 543–546, 1985. 6915

Kerr, J. B., Asbridge, I. A., and Evans, W. F. J.: Intercomparison of total ozone measured by the Brewer and Dobson spectrophotometers at Toronto, J. Geophys. Res., 93, 11 129–11 140,

1988. 6917
Koelemeijer, R. B. A., Stammes, P., Hovenier, J. W., and de Haan, J. F.: A fast method for retrieval of cloud parameters using oxygen A-band measurements from the Global Ozone Monitoring Experiment, J. Geophys. Res., 106, 3475–3496, 2001. 6913, 6914
Koelemeijer, R. B. A., de Haan, J. F., and Stammes, P.: A database of spectral surface reflectivity in the range 335–772 nm derived from 5.5 years of GOME observations, J. Geophys. Res., 108, doi:10.1029/2002JD002429, 2003. 6913
Komhyr, W. D., Mateer, C. L., and Hudson, R. D.: Effective Bass-Paur 1985 ozone absorption coeffcients for use with Dobson ozone spectrophotometers, J. Geophys. Res., 98, 20 451–20 465, 1993. 6917
Kurucz, R. L., Furenlid, I., Brault, J., and Testerman, L.: Solar flux atlas from 296 nm to 1300 nm, National Solar Observatory, Sunspot, New Mexico, 1984. 6914
Laan, E., de Vries, J., Kruizinga, B., Visser, H., Levelt, P., van den Oord, G. H. J., Maelkki, A., Leppelmeier, G., and Hilsenrath, E.: Ozone monitoring with the OMI instrument, in Proceedings of the SPIE SPIE's 45th Annual Meeting – The International Symposium on Optical Science and Technology, vol. 4132-41, 334–343, 2000. 6925
Rozanov, V. V., Kurosu, T., and Burrows, J. P.: Retrieval of Atmospheric Constituents in the UV/visible: A new Analytical Approach to Calculating Weighting Functions, J. Quant. Spectrosc. Rad. Transfer, 60, 277–299, 1998. 6912
Solomon, S., Schmeltekopf, A. L., and Sanders, R. W.: On the interpretation of zenith-sky absorption measurements, J. Geophys. Res., 92, 8311–8319, 1987. 6913
Staehelin, J.: Total ozone series of Arosa (Switzerland), Homogenization and data comparison, J. Geophys. Res., 103, 5827–5841, 1998. 6915
Staehelin, J., Kerr, J., Evans, R., and Vanicek, K.: Comparison of total ozone measurements of Dobson and Brewer spectrophotometers and recommended transfer functions, Tech. rep., WMO, world Meteorological Organization Global Atmosphere Watch (WMO-GAW) Report 149, 2003. 6911, 6915, 6917, 6921, 6924
Tanzi, C. P., Snel, R., Hasekamp, O., and Aben, I.: Degradation of UV earth albedo observations by GOME, in ERS-ENVISAT Symposium, Gothenburg, 16–20 October 2000, eSA Special Publication SP-461 (CD-ROM), 2001. 6923
Vanicek, K.: Differences between Dobson and Brewer observations of total ozone at Hradec-Kralove, in Atmospheric Ozone, Proc. Quadr. Ozone Symp., edited by Bojkov, R. and Visconti, G., 81–84, Edigrafital S.p.A.-S.Atto (TE), 1998. 6918

Vountas, M., Rozanov, V. V., and Burrows, J. P.: Ring Effect: Impact of Rotational Raman Scattering on Radiative Transfer in Earth's Atmosphere, J. Quant. Spectrosc. Radiat. Transfer, 60, 943–961, 1998. 6913

Weber, M., Eichmann, K.-U., Wittrock, F., Bramstedt, K., Hild, L., Richter, A., Burrows, J. P., and Müller, R.: The cold Arctic winter 1995/96 as observed by the Global Ozone Monitoring Experiment GOME and HALOE: Tropospheric wave activity and chemical ozone loss, Quart. J. Roy. Meteorol. Soc., 1293–1319, 2002. 6921

Weber, M., Dhomse, S., Wittrock, F., Richter, A., Sinnhuber, B.-M., and Burrows, J. P.: Dynamical Control of NH and SH Winter/Spring Total Ozone from GOME Observations in 1995–2002, Geophys. Res. Lett., 30, 1853–1854, doi:10.1029/2002GL016799, 2003. 6921

Wellemeyer, C. G., Taylor, S. L., Seftor, C. J., McPeters, R. D., and Bhartia, P. K.: A correction for the Total Ozone Mapping Spectrometer profile shape errors at high latitude, J. Geophys. Res., 102, 9029–9038, 1997. 6912, 6914, 6924

Table 1. List of WOUDC station data used in the WFDOAS validation and division into climate zones.

Station No.	Latitude	Longitude	Height [m]	Location
NH polar region				
024	74.72° N	94.98° W	65	Resolute
199	71.32° N	156.6° W	11	Barrow
105	64.82° N	147.87° W	138	Fairbanks
051	64.13° N	21.9° W	75	Reykjavik
123	62.08° N	129.75° E	98	Yakutsk
043	60.13° N	1.18° W	95	Lerwick
NH mid-latitude region				
077	58.75° N	94.07° W	35	Churchill
143	56.00° N	92.88° E	137	Krasnoyarsk
021	53.55° N	114.10° W	766	Edmonton
076	53.32° N	160.38° W	44	Goose Bay
130	52.97° N	158.75° E	78	Petropavlovsk
174	52.22° N	14.12° E	112	Lindenberg
053	50.80° N	4.35° E	100	Uccle
036	50.22° N	5.32° W	88	Camborne
099	47.80° N	11.02° E	975	H'peissenberg
277	47.73° N	42.25° E	64	Cimljansk
020	46.87° N	68.02° W	192	Caribou
119	46.48° N	30.63° E	42	Odessa
065	43.78° N	79.47° W	198	Toronto
012	43.05° N	141.33° E	19	Sapporo
067	40.02° N	105.25° W	1390	Boulder
208	39.77° N	117.00° E	80	Shiangher
293	39.45° N	22.48° E	110	Athens
107	37.93° N	75.48° W	13	Wallops Island
158	33.57° N	7.67° W	55	Casablanca

ACPD
4, 6909–6941, 2004
GOME WFDOAS total ozone validation
M. Weber et al.

Table 1. Continued.

Tropics				
031	19.53° N	155.57° W	3420	Mauna Loa
187	18.53° N	73.85° E	559	Poona
218	14.63° N	121.83° E	61	Manila
214	1.33° N	103.88° E	14	Singapore
175	1.27° S	36.8° E	1745	Nairobi
219	5.84° S	35.21° W	32	Natal
084	12.42° S	130.88° E	31	Darwin
191	14.25° S	170.56° W	82	Samoa
200	22.68° S	45.00° W	573	C. Paulista
SH mid-latitude				
027	27.42° S	153.12° E	18	Brisbane
343	31.38° S	57.97° W	31	Salto
091	34.58° S	58.48° W	25	Buenos Aires
253	37.80° S	144.97° E	125	Melbourne
256	45.06° S	169.70° E	370	Lauder
342	45.78° S	67.5° W	43	C. Rivadavia
339	54.85° S	68.31° W	7	Ushuaia
Antarctica				
233	64.23° S	56.72° W	196	Marambio
101	69.00° S	39.58° E	21	Syowa
057	73.51° S	26.73° W	31	Halley Bay
268	77.83° S	166.68° E	250	Arrival Heights

ACPD

4, 6909–6941, 2004

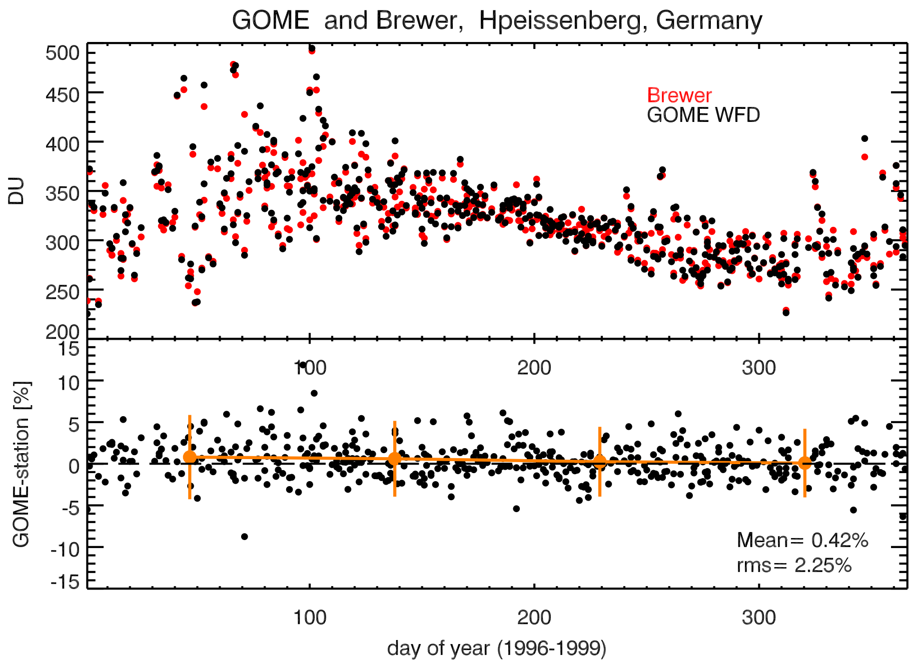

Fig. 1. Top panel: Collocated GOME WFDOAS V1.0 and Brewer total ozone from Hohenpeissenberg. Bottom panel: Differences in percent. Orange points mark the three month average in the daily differences and bars the 2σ RMS from taking the mean.

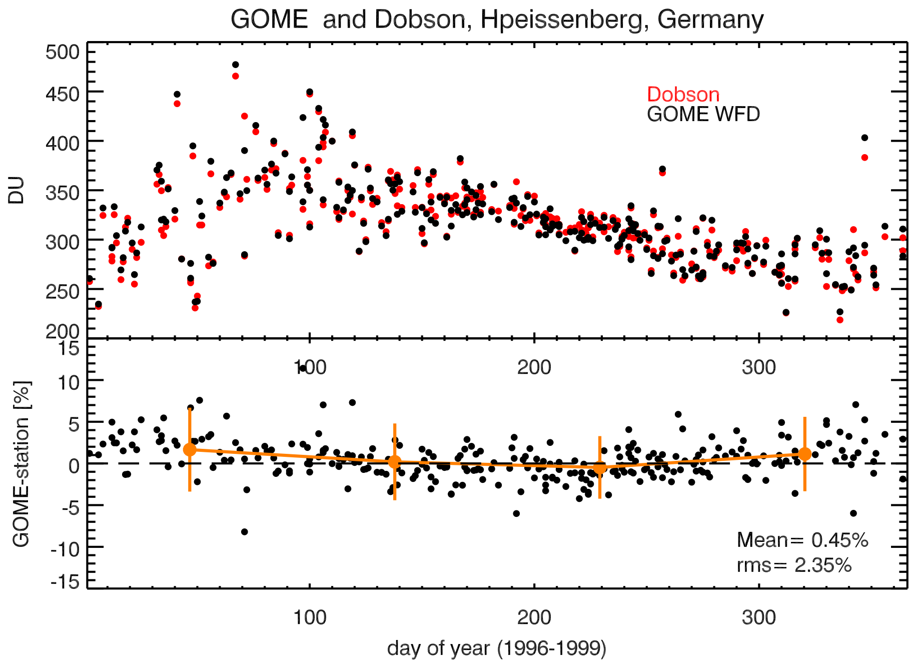

Fig. 2. Same as Fig. 1 but shown for collocated WFDOAS and Dobson measurements at Hohenpeissenberg. Only direct-sun measurements from the Dobson are shown here.

ACPD
4, 6909–6941, 2004

Title Page
Abstract
Introduction
Conclusions
References
Tables
Figures
◀
▶
Back
Close
Full Screen / Esc
Print Version
Interactive Discussion

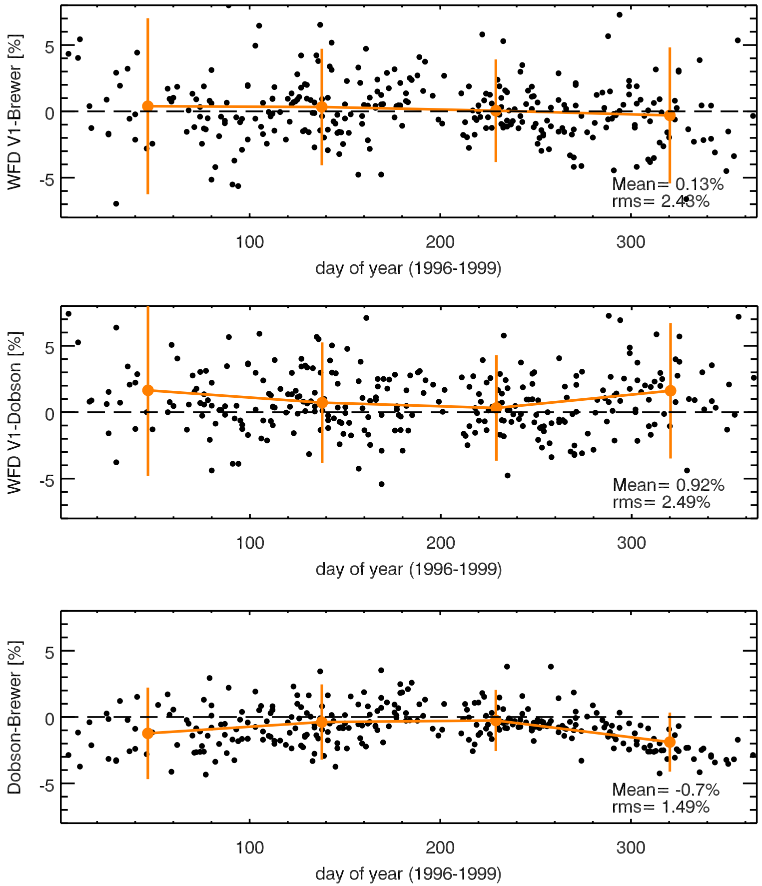

Fig. 3. Annual course of differences between GOME WFDOAS V1, single Brewer, and Dobson data at Hradec-Kralove shown for all possible pair combinations. Top: WFDOAS minus Brewer. Middle: WFDOAS minus Dobson, Bottom: Dobson minus Brewer.

ACPD

4, 6909–6941, 2004

GOME WFDOAS total ozone validation

M. Weber et al.

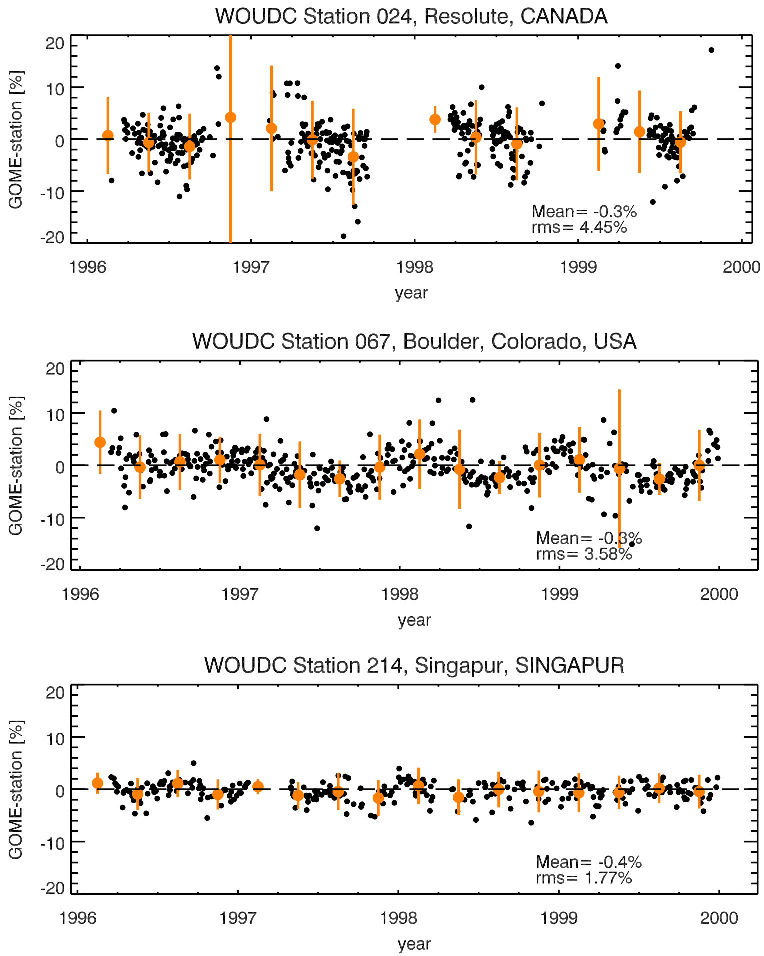

Fig. 4. Daily differences between collocated GOME WFDOAS V1.0 and various Dobson stations distributed from north to south between 1996 and 1999. Orange points mark three month averages and error bars the 2σ RMS in the observed differences.

ACPD

4, 6909–6941, 2004

GOME WFDOAS total ozone validation

M. Weber et al.

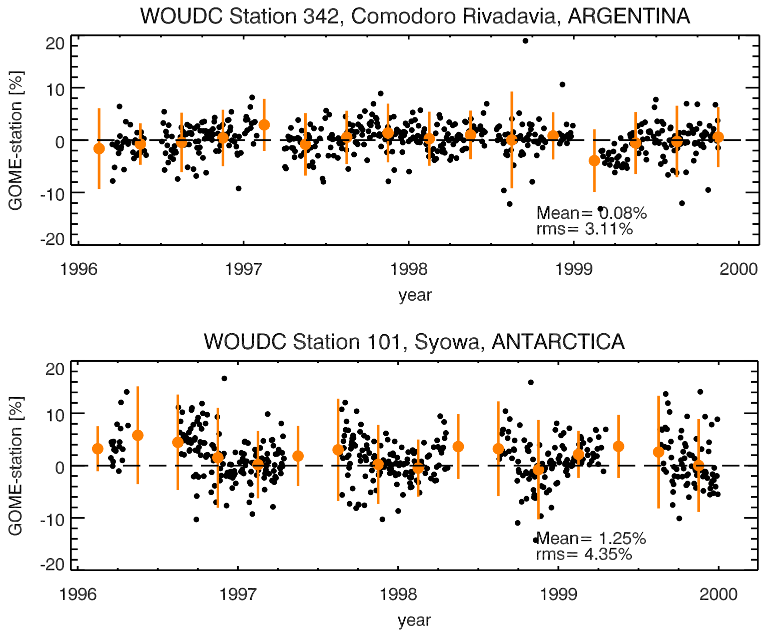

Fig. 4. Continued.

ACPD
4, 6909–6941, 2004

GOME WFDOAS total ozone validation

M. Weber et al.

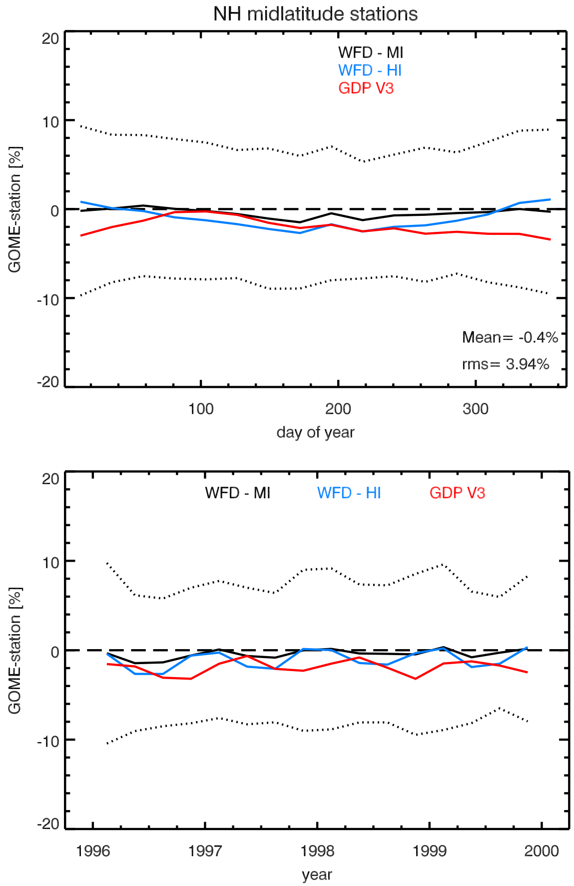

Fig. 5. Average of WFDOAS V1.0 and GDP V3.0 differences to nineteen NH mid-latitude WOUDC stations: 1996–1999. Top: annual course, bottom: all years. WFD-MI refers to mid-latitude a-priori ozone profile climatology and WFD-HI to high-latitude profiles. Black lines refer to the default retrieval (here WFD-MI) and 2σ RMS in differences.

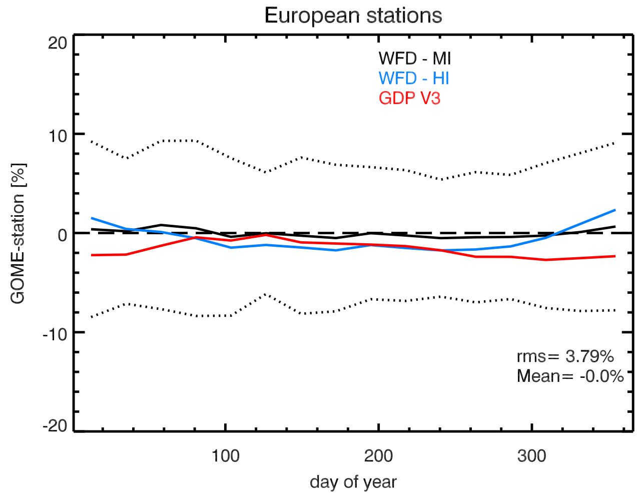

Fig. 6. Same as Fig. 5, but for eight European stations (Arosa, Lindenberg, Potsdam, Hohenpeissenberg, Hradec-Kralove, Uccle, Camborne, and Oslo), see text for further details.

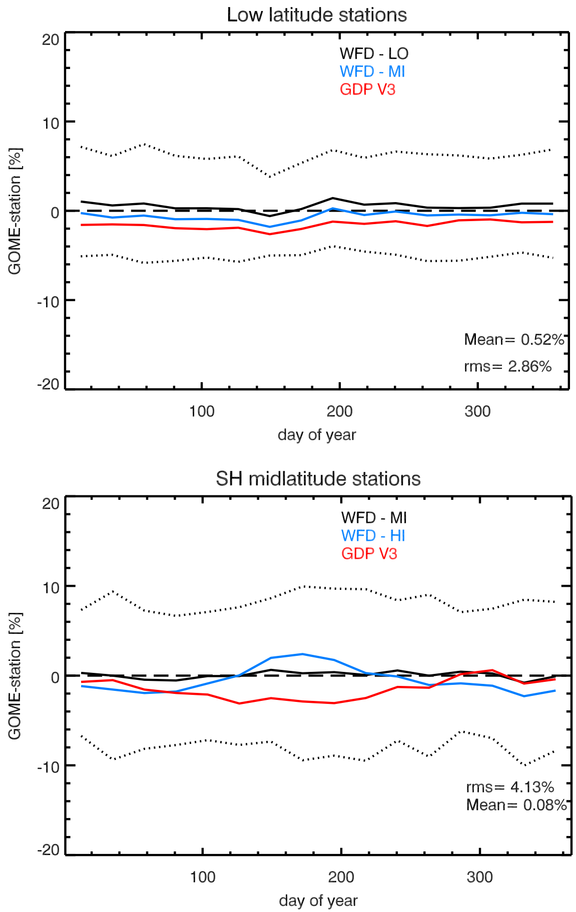

Fig. 7. Annual course of differences between GOME and ground stations for tropics (top) and SH mid latitudes (bottom). The default retrieval (black lines) is WFD-MI at mid latitudes and WFD-LO in the tropics.

ACPD
4, 6909–6941, 2004

GOME WFDOAS total ozone validation

M. Weber et al.

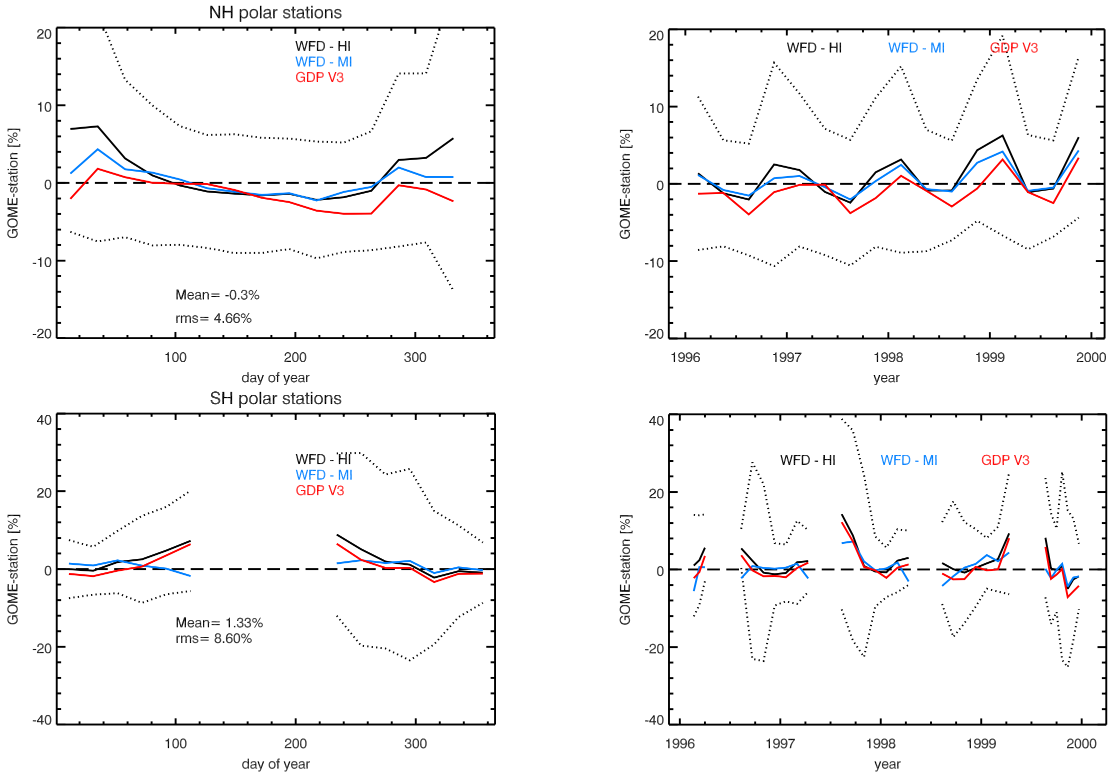

Fig. 8. Mean differences between GOME and ground stations for polar latitudes. Top: NH stations as a function of day of year (left) and time (right). Bottom: SH stations as a function of day of year (left) and time (right). Default retrieval here is WFD-HI (black lines).

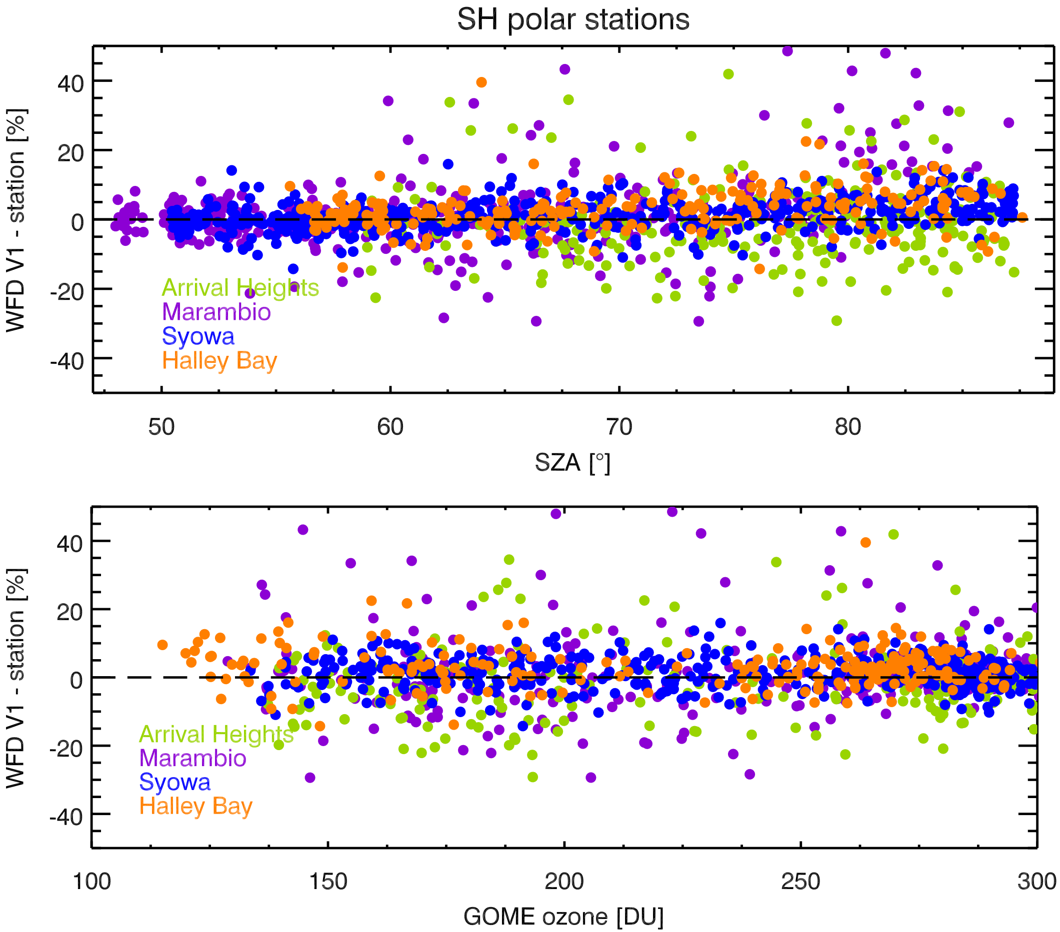

Fig. 9. WFDOAS V1 minus Dobson total ozone as a function of solar zenith angle (top) and GOME total ozone (bottom) for four SH polar stations: Arrival Heights (78° S), Halley Bay (74° S), Syowa (69° S), and Marambio (64° S).

ACPD
4, 6909–6941, 2004

GOME WFDOAS total ozone validation

M. Weber et al.

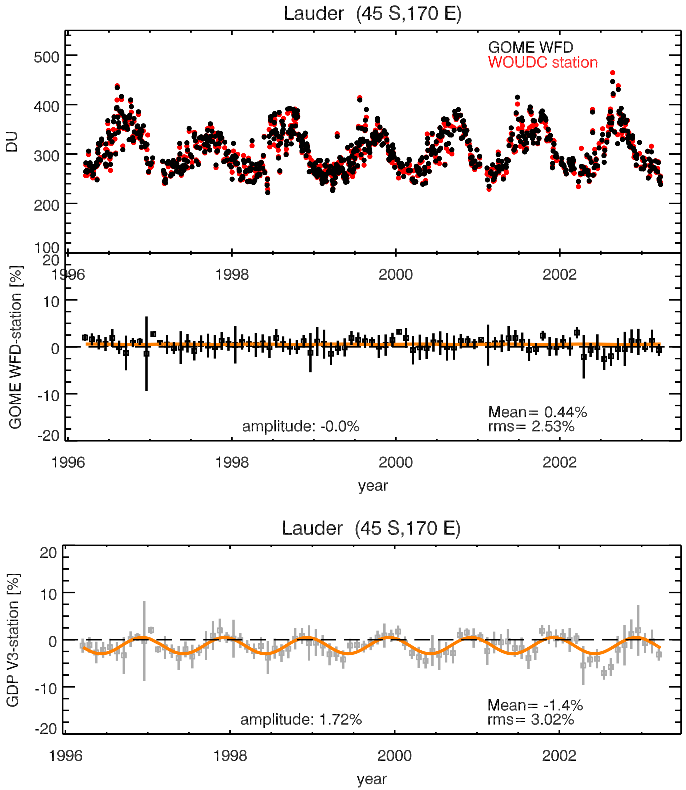

Fig. 10. Longterm comparison between GOME and Lauder Dobson. Top: daily collocated GOME WFDOAS (black) and Dobson data (red) time series. Middle panel: monthly mean differences between WFDOAS and Lauder Dobson in percent. Bottom: same as middle panel, but for GOME GDP V3. Vertical bars indicate the 1σ RMS of the daily differences. Orange lines in bottom two panels show the cosine fit to the data to determine the amplitude of the seasonal variation. The amplitude of the cosine term is 0% and 1.7% for GOME WFDOAS and GDP V3.0, respectively.

ACPD
4, 6909–6941, 2004

GOME WFDOAS total ozone validation

M. Weber et al.